Electronic Supplementary Material (ESI) for Journal of Materials Chemistry C.

Understanding Surface Chemistry during $MAPbI_3$ Spray Deposition and its Effect on Photovoltaic Performance

Conor Rocks,,[a] Paul Maguire,[a] Vladimir Svrcek,[b] and Davide Mariotti *,[a]*

Supporting Information

Additional X-ray photoelectron spectroscopy (XPS) Spectra. The XPS survey spectrum for a typical $MAPbI_3$ perovskite shows peaks at binding energies of 284.8 eV, 401 eV and 532 eV corresponding to the photoelectron peaks of C 1s, N 1s and O 1s respectively. The doublet peaks of I and Pb are located around 618 eV and 137 eV, respectively, with their associated spin orbit splitting (Figure S1).

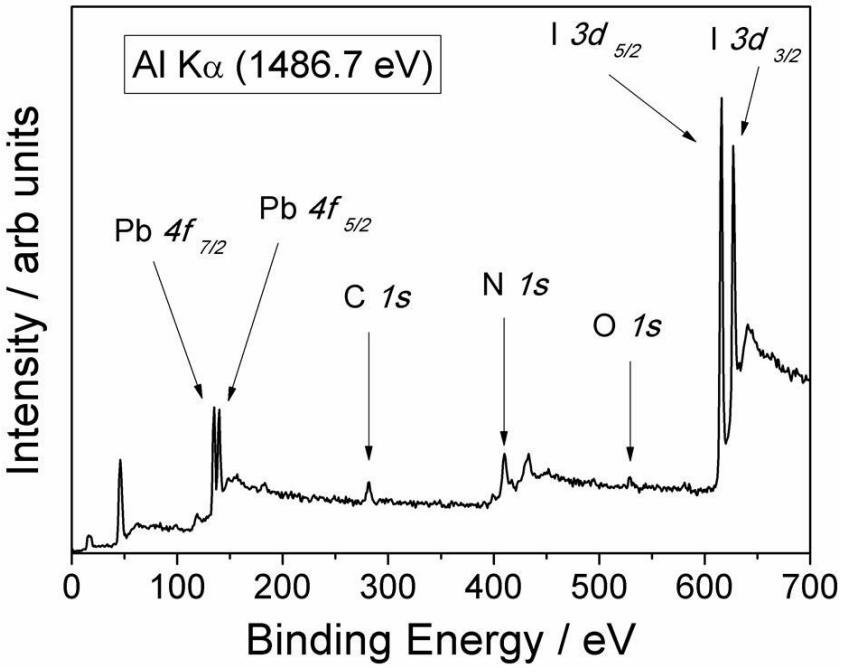

Fig S1: XPS survey spectrum for $MAPbI_3$ perovskite film (I/Pb atomic mass ratio = 3:1).

Figure S2 shows XPS core level spectra for N *1s* where a-f represents decreasing $MAPbI_3$ film thickness and highlights the destruction of the perovskite organic (CH_3-NH_3) core close to the surface for thin $MAPbI_3$ films. From the N *1s* core level spectra of the same $MAPbI_3$ films there are two peaks present at 399.9 eV and 401.6 eV, corresponding to the existence of free amine group NH_x and NH_2 singly bonded to carbon respectively.[1,2] It is interesting to note the existence of NH_2 bond even in the thicker $MAPbI_3$ films where the I/Pb ratio is ~3:1. This indicates that the organic core (CH_3NH_3) is decomposed due to weak hydrogen bonds, resulting in the deprotonation of NH_3 to NH_2.[3] Decreasing $MAPbI_3$ film thickness reduces the concentration of the methyl component through evaporation of MAI (CH_3NH_2I) until the organic species is not present at the surface (< 10 nm) of our films, with atomic ratio I/Pb reducing towards to 2:1. The rapid surface chemistry observed for thin $MAPbI_3$ films can be compared with typical chemical decomposition that is expected under prolonged aging in ambient conditions.

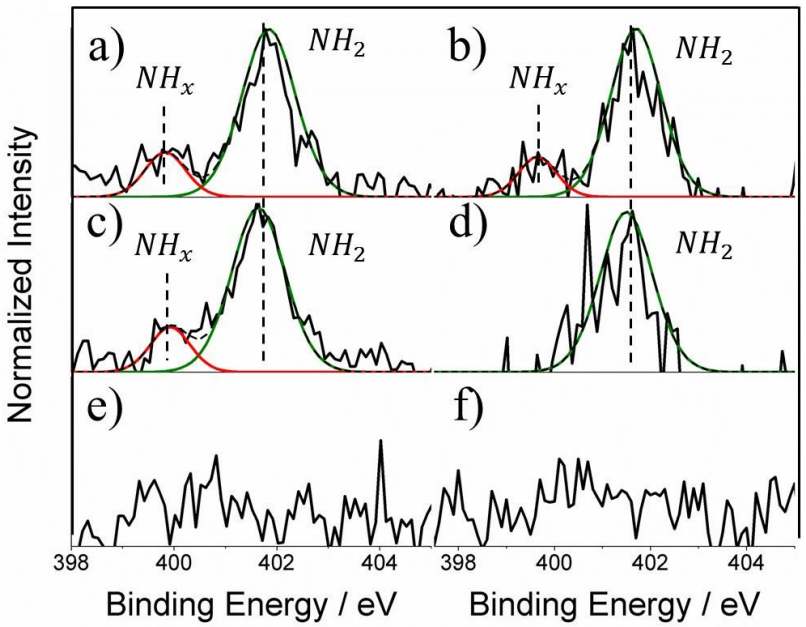

Fig S2: X-ray photoelectron core level spectra for N *1s* where a-f) represents decreasing $MAPbI_3$ film thickness: a)4.99 μm, b) 4.65 μm, c) 2.67 μm, d) 1.71 μm, e) 1.37 μm and f) 0.67 μm.

Prolonged Aging of $MAPbI_3$ Films in Atmosphere. Figure S3 shows FTIR spectra for a separate $MAPbI_3$ film that has undergone prolonged aging (30 days) with a number of clearly defined peaks within the region 800-3200 cm^{-1}, commonly assigned to vibrations of the MA cations. Peaks named (a.-b.) and located around 800 cm^{-1} and 900 cm^{-1} in the figure correspond to CH_3-NH_3 rocking modes with a shoulder peak (c.) at 960 cm^{-1} assigned to a C-N stretching mode. Additional peak (d.) in the lower infrared region of the spectra, located at 1232 cm^{-1}, is also due to CH_3-NH_3 rocking mode. Higher frequency region (2600-3200 cm^{-1}) displays a number of peaks that have merged to form a broad structure. Peaks located at 3030 cm^{-1}, 3080 cm^{-1}, 3124 cm^{-1} and 3172 cm^{-1} that would be clearly distinguishable in orthorhombic $MAPbI_3$ and linked to C-H and N-H stretching modes combine to form the broad peaks (g.-i.) in the spectra below. Peaks (e.-f.) located around 2700 cm^{-1} and 2820 cm^{-1} are further bending and rocking modes of MA cation. After 30 days aging of the $MAPbI_3$ film, a large decrease in transmittance of these modes is observed. The decrease in MA^+ vibrational modes in FTIR spectra agrees with our XPS data where N and I atomic concentration decrease significantly as a consequence of increased adsorption of atmospheric species.

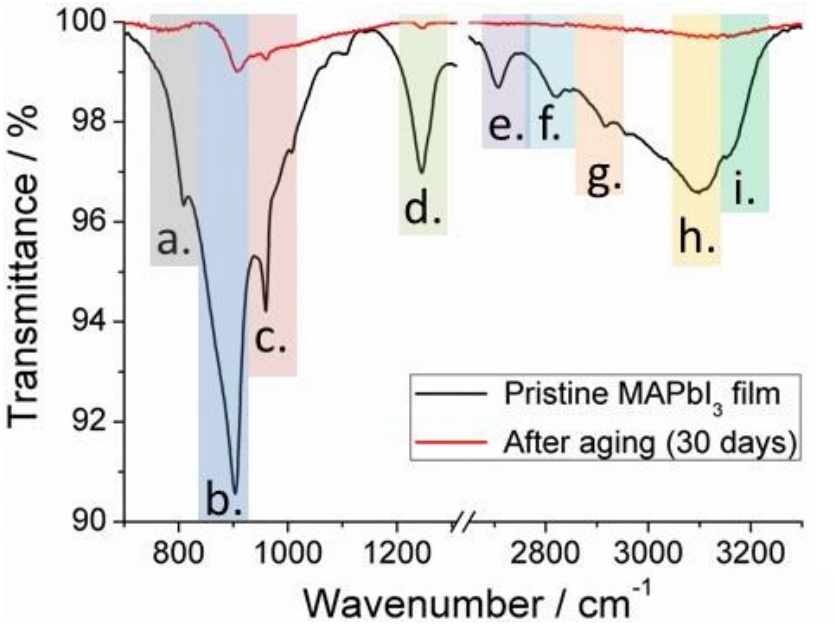

Fig S3: Fourier transform infrared transmittance spectra for a thick $MAPbI_3$ film (I/Pb 3:1) and after 30 days aging in normal atmospheric conditions.

Absorption coefficient measurements were taken from transmission spectra (T) for $MAPbI_3$ films of varying thickness (d) where, on the assumption that reflection can be considered negligible, absorption coefficient (α) is equal to $-\ln(T)/d$. Absorption coefficients for $MAPbI_3$ films have been presented (Figure S4a-f) along with additional spectra showing aged films over time. A typical sharp band edge around 1.55 eV is observed that corresponds to the direct bandgap of the pristine perovskite films.[4] Decreasing $MAPbI_3$ film thickness changes the typical absorption spectra which flattens at the higher energies (Figure S4c-f). Also shown is the effect of continued aging for separate samples (aged film and fully degraded film) where absorption band edge at 1.55 eV severely reduces as a consequence. The resultant PbI_2 band edge at 2.4 eV dominates the absorption until the band-edge associated with $MAPbI_3$ completely disappears.[5]

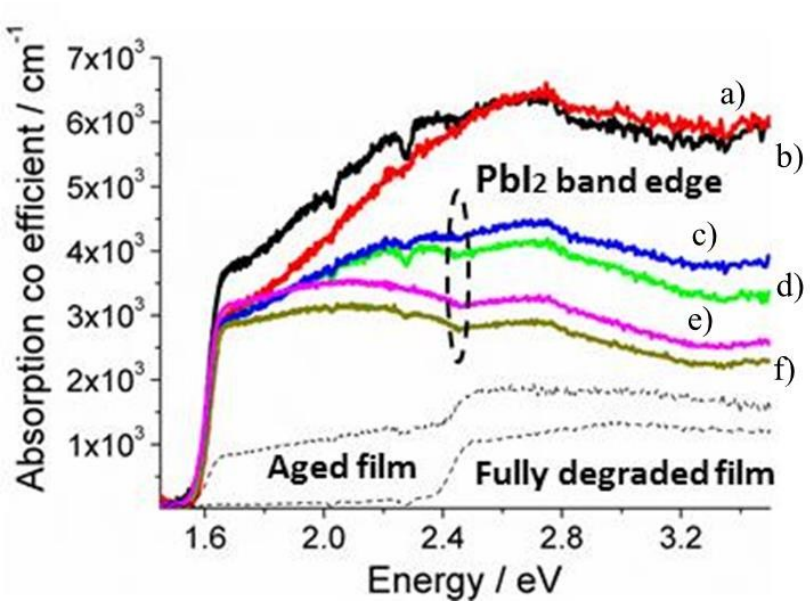

Fig S4: Absorption coefficient for $MAPbI_3$ films with decreasing film thickness: a) 4.99 µm, b) 4.65 µm, c) 2.67 µm, d) 1.71 µm, e) 1.37 µm, f) 0.67 µm.

Raman spectroscopy. Supplementary to FTIR analysis of the organic cation (MA^+) vibrations in $MAPbI_3$ and aging in atmospheric conditions, additional information can be gained from lower frequency region < 200 cm^{-1} where both internal vibrations of PbI_3 network and MA cation can be observed concurrently. Raman spectra for pristine a $MAPbI_3$ film before and after aging in atmosphere are shown (Figure S5). Specifically, vibrations of MA cations have been demonstrated to have significant infrared intensity in the region 140-180 cm^{-1} with internal vibrations of PbI_3 network provides information < 140 cm^{-1}. Raman spectra for pristine $MAPbI_3$ film in figure S5a shows a prominent peak at 147 cm^{-1} that can be attributed to the rotational mode of the organic MA cation with another small peak at 94 cm^{-1} that is assigned to the Pb-I stretching mode in PbI_3 network. The broad background between both peaks may be caused by low intensity modes linked to an additional Pb-I stretching mode at 112 cm^{-1} and the spinning mode of MA cation at 124 cm^{-1}, although the latter has been shown to have minimal Raman activity. Aging of a $MAPbI_3$ film for 30 days

in atmospheric conditions shows very weak intensity MA modes when compared with the Pb-I modes that become visibly more defined in figure S5b. The three main bands for in the PbI_3 inorganic octahedron occurring at 73 cm^{-1}, 97 cm^{-1} and 112 cm^{-1} and are consistent with stretching modes of Pb-I observed in literature for PbI2 at room temperature.[6,7]

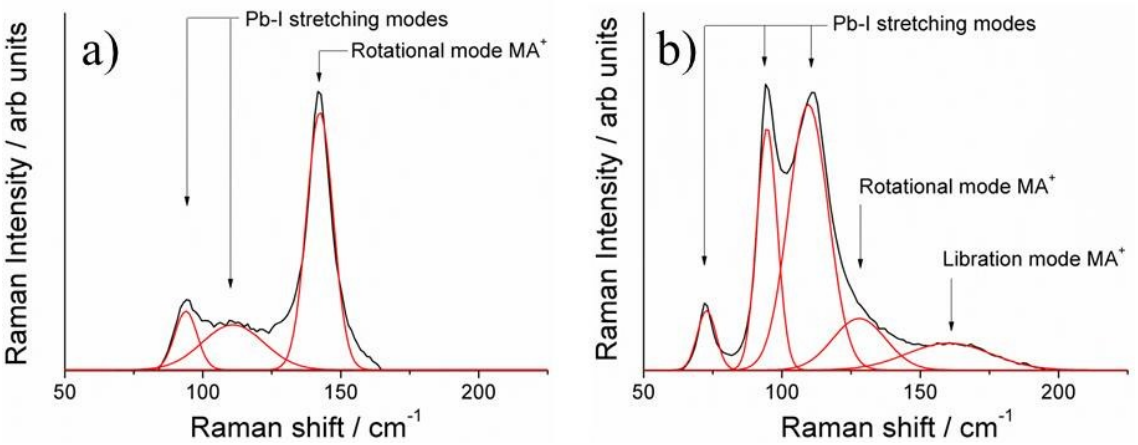

Fig S5: Raman spectroscopy of a) pristine $MAPbI_3$ film and b) after 30 days aging in ambient atmospheric conditions.

SEM of sprayed films (< 500 nm). Reducing the film thickness further to < 500 nm using spray technique proved difficult and produced extremely porous films exhibiting small rod like structures assumed to be PbI_2, highlighted in Figure S6 below. Figure S6 a-b still exhibit the outline of large grain structures however it becomes evident that these large grains have begun to de-agglomerate due to the chemical decomposition (Figure S6c-d). The incorporation of these low thickness films in PV devices resulted in shunting behaviour due to the non-homogeneity of the sprayed film (not shown). The rapid degradation for thin sprayed films (< 500 nm) is in good agreement with the surface chemical gradient determined within main manuscript for decreasing $MAPbI_3$ films (Figure 2,4 and 5). In order to fabricate high efficiency devices that are more technologically relevant, using this one step spray

technique, the issue of rapid degradation observed in thin films will need to be addressed and overcame.

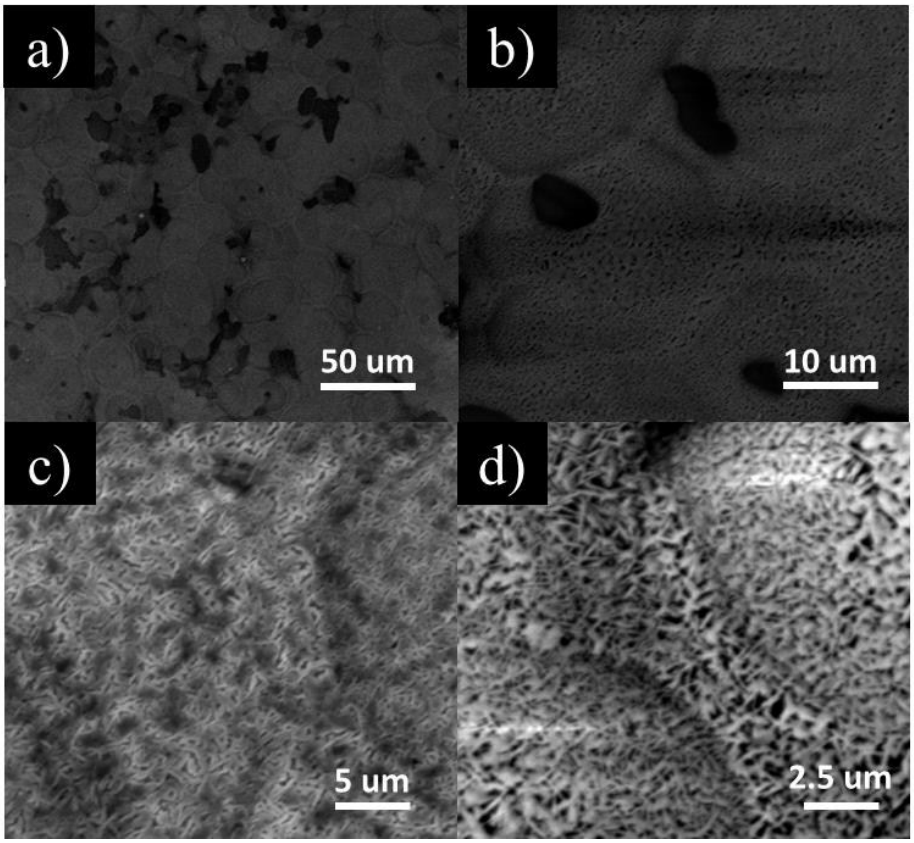

Fig S6: a-d) scanning electron microscopy of spray deposited $MAPbI_3$ film (< 500 nm) where rapid chemical decomposition has occurred resulting in a highly porous film due to the formation of rod like PbI_2 structures.

Equivalent circuit diagram

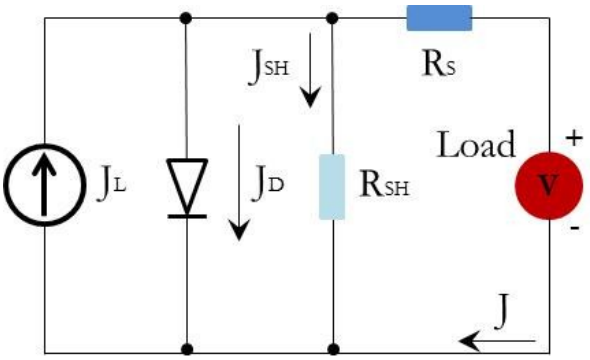

Fig S7: Ideal model for a single heterojunction solar cell with: J_D (current of pn-junction diode), J_L (light induced constant current), J_{SH} (the shunt current), R_S (the series resistance), R_{SH} (the shunt resistance) and J (the current flowing through the external load).

Photovoltaic Performance under light soaking

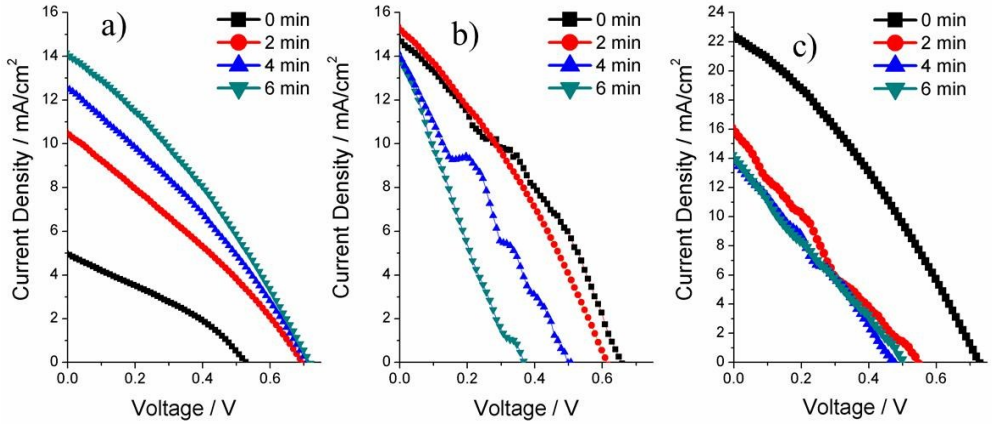

Fig S8: Current voltage curves for $MAPbI_3$ devices film thickness a) 4.99 µm b) 2.67 µm and c) 0.67 µm subject to increasing time under illumination

A	Current voltage (IV) parameters			
Time (mins)	Voc	FF	n %	Jsc
0	0.52	0.3	0.84	4.95
2	0.69	0.28	2.12	10.46
4	0.7	0.3	2.72	12.61
6	0.71	0.31	3.21	14.12
B	Current voltage (IV) parameters			
Time (mins)	Voc	FF	n %	Jsc
0	0.66	0.31	2.94	14.76
2	0.61	0.33	3.28	15.28
4	0.5	0.29	2.07	14.12
6	0.36	0.3	2.08	13.77
C	Current voltage (IV) parameters			
Time (mins)	Voc	FF	n %	Jsc
0	0.73	0.32	5.23	22.47
2	0.54	0.24	2.15	16.01
4	0.47	0.27	1.75	13.56
6	0.49	0.25	1.33	13.99

Table 1: Current voltage parameters for curves a-c) displayed in Figure S6 subject to continued illumination 0-6 minutes.

References:

(1) Rajendra Kumar, G.; Dennyson Savariraj, A.; Karthick, S. N.; Selvam, S.; Balamuralitharan, B.; Kim, H.-J.; Viswanathan, K. K.; Vijaykumar, M.; Prabakar, K. Phase Transition Kinetics and Surface Binding States of Methylammonium Lead Iodide Perovskite. *Phys. Chem. Chem. Phys.* **2016**, *18* (10), 7284–7292.

(2) Naphade, R.; Nagane, S.; Shanker, G. S.; Fernandes, R.; Kothari, D.; Zhou, Y.; Padture, N. P.; Ogale, S. Hybrid Perovskite Quantum Nanostructures Synthesized by Electrospray Antisolvent–Solvent Extraction and Intercalation. *ACS Appl. Mater.*

Interfaces **2016**, *8* (1), 854–861.

(3) Ren, Y.; Oswald, I. W. H.; Wang, X.; McCandless, G. T.; Chan, J. Y. Orientation of Organic Cations in Hybrid Inorganic–Organic Perovskite CH 3 NH 3 PbI 3 from Subatomic Resolution Single Crystal Neutron Diffraction Structural Studies. *Cryst. Growth Des.* **2016**, *16* (5), 2945–2951.

(4) Cui, D.; Yang, Z.; Yang, D.; Ren, X.; Liu, Y.; Wei, Q.; Fan, H.; Zeng, J.; Liu, S. (Frank). Color-Tuned Perovskite Films Prepared for Efficient Solar Cell Applications. *J. Phys. Chem. C* **2016**, *120* (1), 42–47.

(5) Finlayson, C. E.; Sazio, P. J. A. Highly Efficient Blue Photoluminescence from Colloidal Lead-Iodide Nanoparticles. *J. Phys. D. Appl. Phys.* **2006**, *39* (8), 1477–1480.

(6) Zhou, Y.; Garces, H. F.; Padture, N. P. Challenges in the Ambient Raman Spectroscopy Characterization of Methylammonium Lead Triiodide Perovskite Thin Films. *Front. Optoelectron.* **2016**, *9* (1), 81–86.

(7) Jain, S. M.; Philippe, B.; Johansson, E. M. J.; Park, B.; Rensmo, H.; Edvinsson, T.; Boschloo, G. Vapor Phase Conversion of PbI 2 to CH 3 NH 3 PbI 3 : Spectroscopic Evidence for Formation of an Intermediate Phase. *J. Mater. Chem. A* **2016**, *4* (7), 2630–2642.